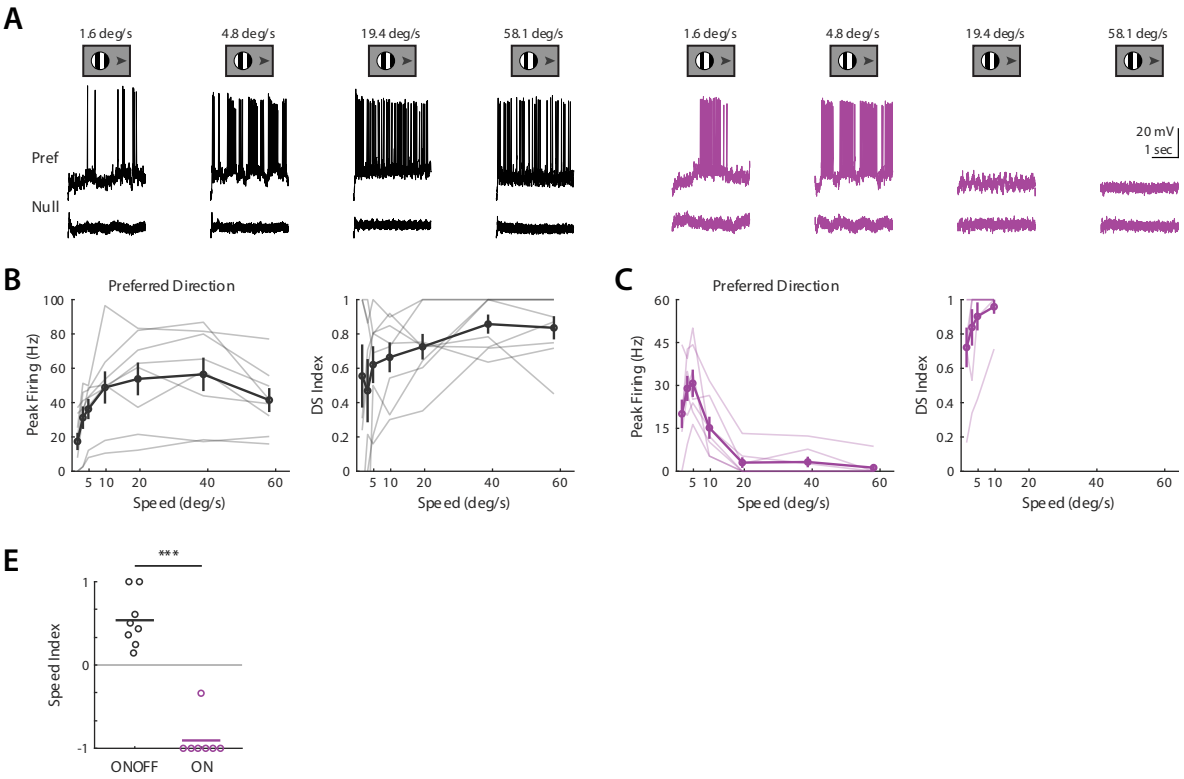

Figure S1. Velocity tuning of DSGCs not altered by using drifting gratings, related to Figure 1

(A) Example current clamp recordings *(ON-OFF black, ON purple*) in response to gratings drifting at several temporal frequencies in the cell's preferred or null direction. (B) ON-OFF DSGC dependence of preferred direction spiking (*left*) and directional selectivity (*right*) on grating velocity. (C) Same as in B, but for ON DSGCs. Directional selectivity is difficult to assess at high velocities due to low overall spiking. (E) Speed tuning indices of preferred direction spiking. Comparison made via two-sided Wilcoxon rank-sum test; ***$P = 3.1 \times 10^{-4}$, 8 ON-OFF DSGCs in 5 mice, 7 ON DSGCs in 6 mice.

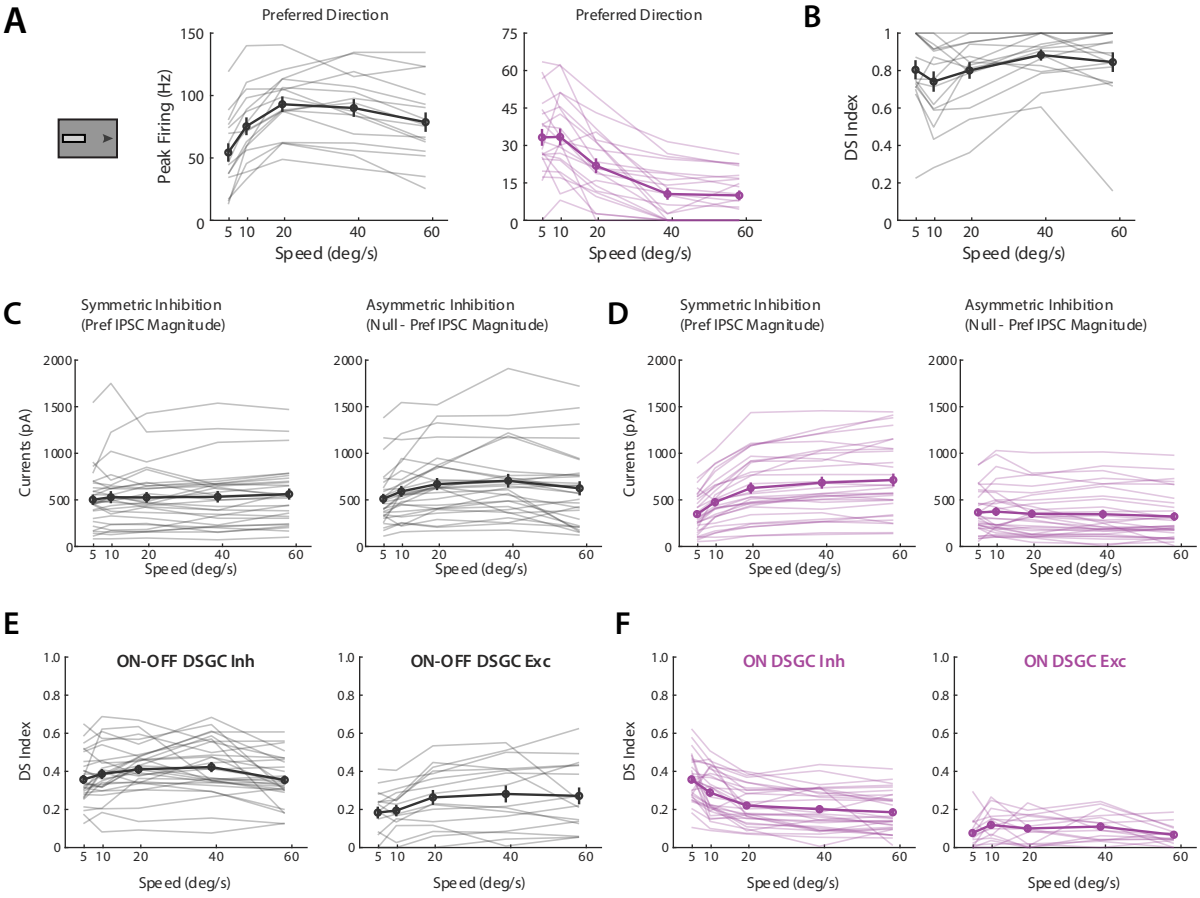

Figure S2. Data for Figures 1-3 presented as unnormalized values, related to Figures 1-3
(A) Summary plot of unnormalized velocity tuning curves based on current clamp recordings of ON-OFF (*black*) and ON DSGCs (*purple*) in response to drifting bar stimuli. In this and all other panels, transparent lines show individual cells while bold lines are the population average. Error bars show standard error of the mean. (B) ON-OFF DSGC direction selectivity indices versus velocity. ON DSGC directional selectivity is difficult to assess at high velocities due to low overall spiking and so is not included. (C) Summary plot of unnormalized velocity tuning curves of ON-OFF DSGC symmetric (*left*) and asymmetric (*right*) inhibition based on voltage clamp recordings. Symmetric inhibition was defined as the amplitude of preferred direction IPSCs, while asymmetric inhibition was measured as the amplitude of null direction IPSCs minus the magnitude of symmetric inhibition. (D) Same as in C, but for ON DSGCs. (E) ON-OFF DSGC direction selectivity indices of synaptic inputs versus velocity. Direction selectivity indices calculated directly from preferred versus null IPSC (*left*) and EPSC (*right*) amplitudes. (F) Same as E, but for ON DSGCs.

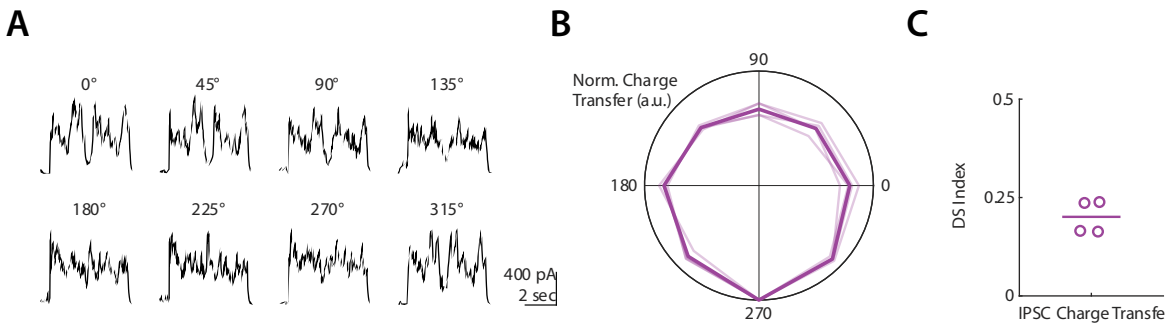

Figure S3. ON DSGC IPSCs for 25 deg/sec random dot kinetograms show directional tuning, related to Figures 1-2

(A) Example ON DSGC inhibitory postsynaptic currents (IPSCs) for random dot kinteogram (RDK) stimuli moving coherently in one of eight directions. (B) Polar plot directional tuning curves of ON DSGCs normalized inhibitory charge transfer for RDK stimuli. Directions of maximal inhibition are aligned to 270 degrees. Transparent lines are tuning of individual cells, bold line is population average. (C) Direction selective indices computed from inhibitory charge transfer.

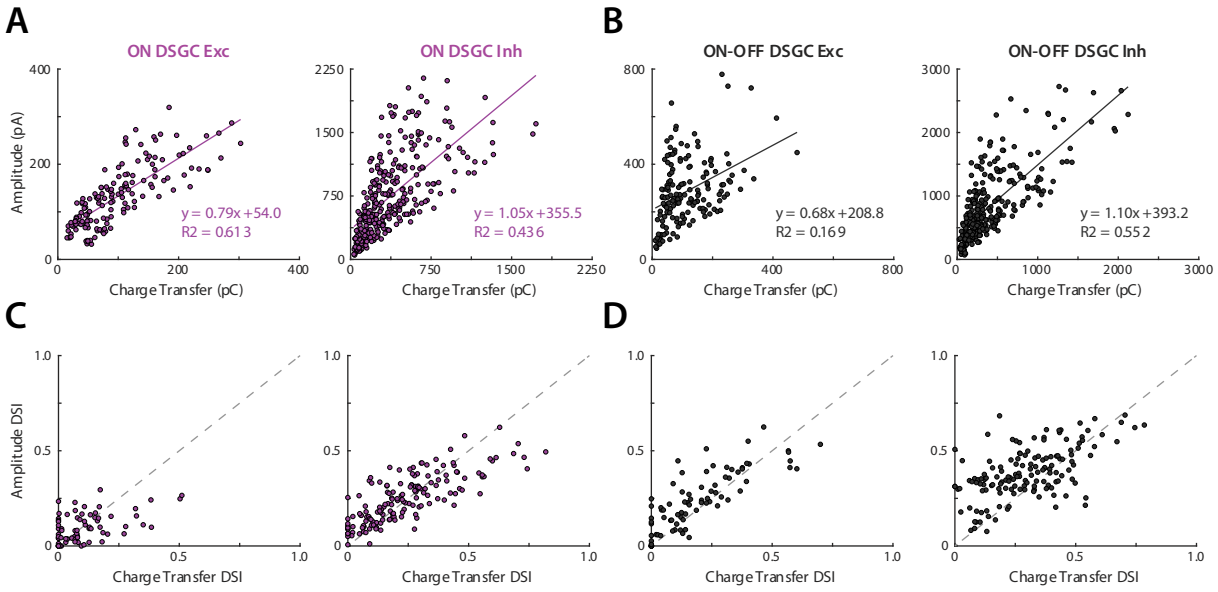

Figure S4. Total synaptic input is well approximated by EPSC and IPSC amplitudes, related to Figures 2-3

(A) Relationship between ON DSGC EPSC (*left*) / IPSC (*right*) amplitude and charge transfer. Individual points are the mean values for a given cell at a set velocity. Solid lines are linear fits, with slope, intercept, and coefficient of determination inset. (B) Same as a, but for ON-OFF DSGCs. (C) Relationship between ON DSGC direction selectivity of EPSC (*left*) / IPSC (*right*) amplitude and charge transfer. Individual points are the value for a given cell at a set velocity. Dashed gray line is unity. (D) Same as C, but for ON-OFF DSGCs.

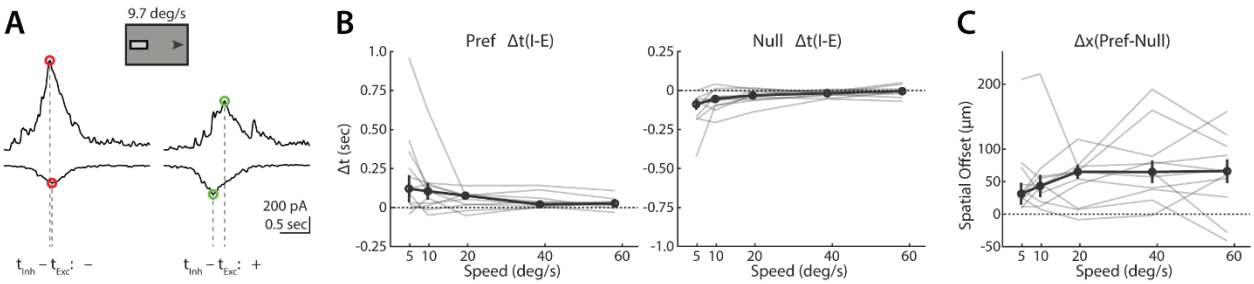

Figure S5. Method for determining the relative timing differences between excitation and inhibition, related to Figures 2-3 and 5

(A) Example ON-OFF DSGC IPSCs (*top*) and EPSCs (*bottom*) illustrating relative timing differences for preferred (*right*) and null (*left*) directed stimuli. IPSC peaks preceding EPSC peaks are treated as negative timing differences, while EPSCs preceding IPSCs are treated as positive timing differences. (B) Dependence of ON-OFF DSGC I-E timing differences on velocity for preferred (*left*) and null (*right*) directed stimuli. Transparent lines show individual cells, bold line is population average. Error bars show standard error of the mean. (C) Directionally tuned component of timing differences represented as a spatial offset. Transparent lines show individual cells, bold line is population average. Error bars show standard error of the mean.

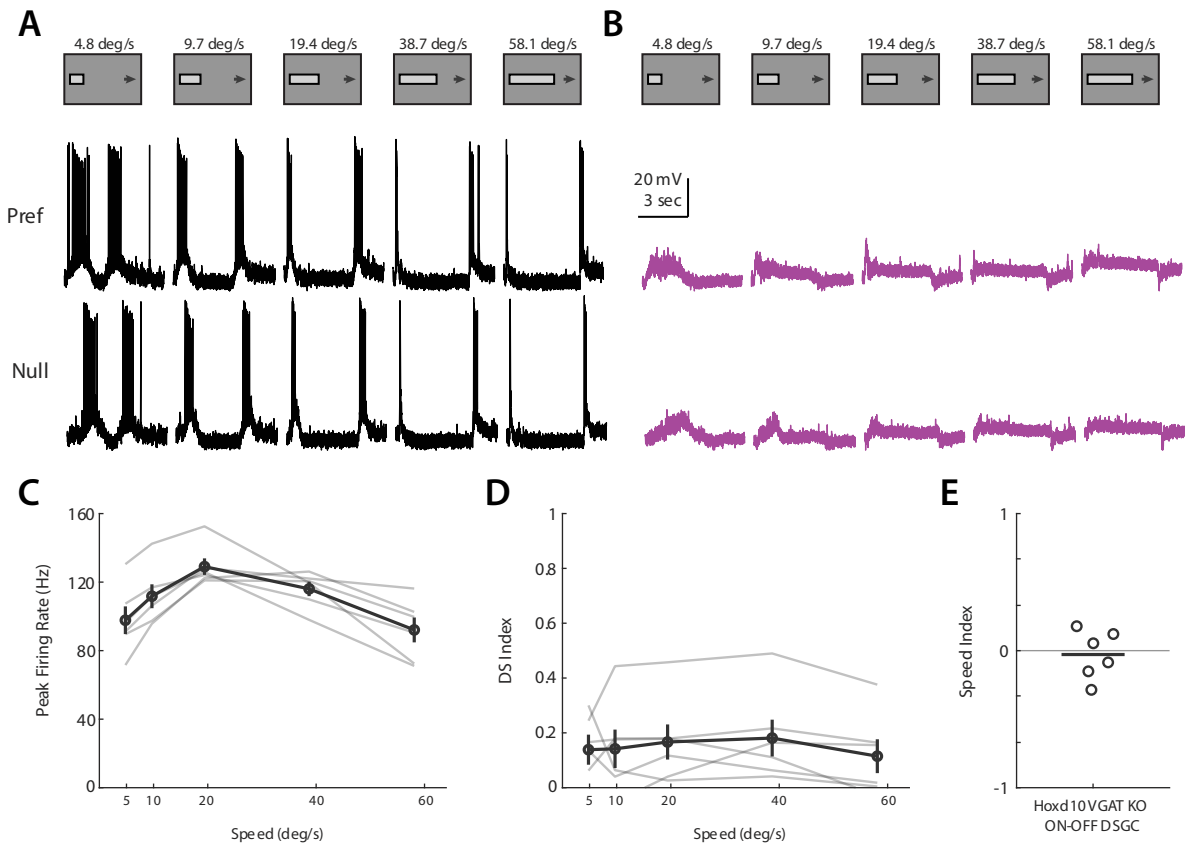

Figure S6. Conditional knockout of starburst amacrine cell vesicular GABA transporters reduces directional spike tuning in ON-OFF DSGCs, related to Figure 6

(A) Example ON-OFF DSGC current clamp recordings in *Hoxd10-GFP / Vgat*$^{flox/flox}$*/ Chat-IRES-Cre* animals. Spiking increases for null direction stimuli relative to wildtype animals, resulting in impaired directional tuning. (B) Example ON DSGC current clamp recording in knockout mouse. Visual stimuli failed to consistently elicit spiking responses in ON DSGCs. (C) Dependence of ON-OFF DSGC preferred direction spiking on drifting bar velocity in knockout animals. Transparent lines show individual cells, bold line is population average. Error bars show standard error of the mean. (D) Same as (C), but for the relationship between direction selectivity and bar velocity. (E) Speed tuning indices of preferred direction spiking.

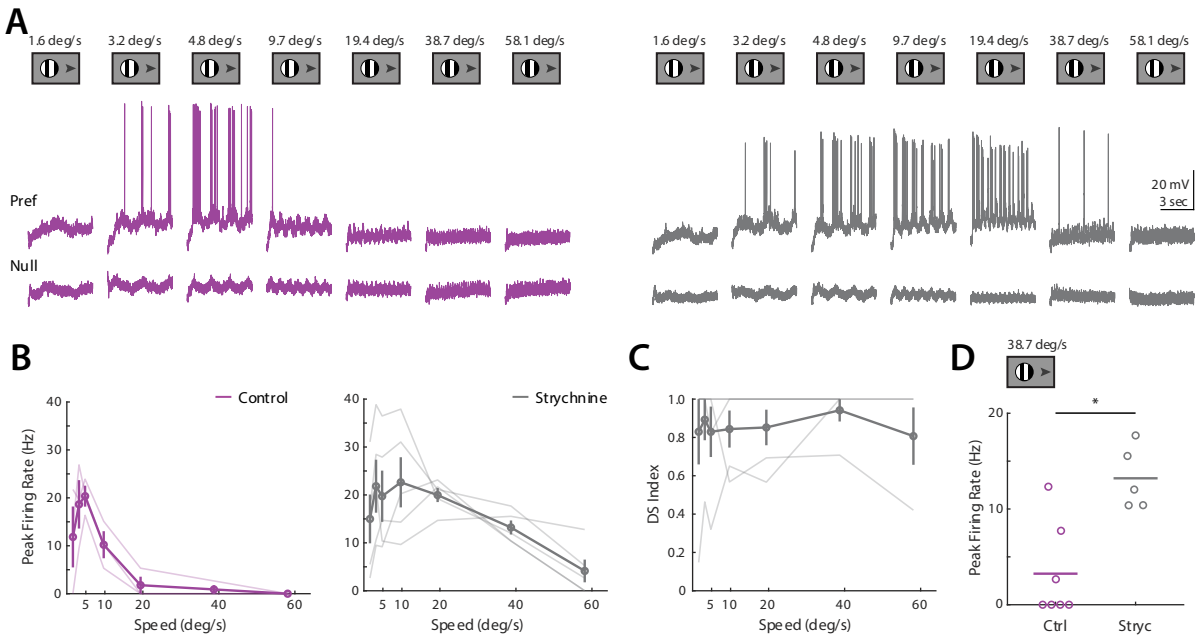

Figure S7. Glycine receptor antagonist strychnine increases ON DSGC spiking at high velocities, related to Figure 7

(A) Example ON DSGC current clamp recordings for gratings drifting at several temporal frequencies in the cell's preferred or null direction, both before (*purple, left*) and after (*gray, right*) strychnine wash. (B) Dependence of preferred direction peak firing rate on drifting grating velocity, before (*left*) and after (*right*) strychnine wash. Transparent lines show individual cells, bold line is population average. Error bars show standard error of the mean. (C) Dependence of direction selectivity index on drifting grating velocity after strychnine wash. Transparent lines show individual cells, bold line is population average. Error bars show standard error of the mean. (D) Comparison of peak preferred direction firing rate at the second highest tested velocity (38.7 deg/sec) in control and strychnine conditions. Lines indicate cells for which recordings both before and after wash were collected. Comparison made via two-sided Wilcoxon rank-sum test; **P* = 0.02, control 7 cells in 6 mice, strychnine 5 cells in 3 mice.

Cell Type	Measure	Condition	Mean	Std Dev	P Value	Cells	Mice
ON-OFF	Spikes	Bars	0.21	0.23	3.8×10^{-3}	16	11
ON-OFF	Spikes	Gratings	0.54	0.32	0.01	8	5
ON	Spikes	Bars	-0.63	0.28	8.4×10^{-5}	21	17
ON	Spikes	Gratings	-0.91	0.25	0.02	7	6
ON-OFF	Sym. Inh.	Bars	0.07	0.15	0.04	29	19
ON-OFF	DS Inh.	Bars	0.06	0.21	0.05	29	19
ON-OFF	Sym. Exc.	Bars	0.09	0.22	0.09	16	10
ON-OFF	DS Exc.	Bars	0.18	0.53	0.18	16	10
ON	Sym. Inh.	Bars	0.36	0.16	1.2×10^{-6}	31	22
ON	DS Inh.	Bars	-0.13	0.21	3.1×10^{-3}	31	22
ON	Sym. Exc.	Bars	-0.09	0.11	0.01	15	10
ON	DS Exc.	Bars	-0.17	0.68	0.39	15	10
ON	Sym. Inh.	Bars, Strychnine	0.10	0.29	0.52	11	8
ON-OFF	Sym. Inh.	Bars, VGAT KO	0.02	0.10	0.62	12	5
ON	Sym. Inh.	Bars, VGAT KO	0.34	0.07	9.7×10^{-4}	11	6
ON-OFF	Spikes	Dynamic Clamp	0.35	0.13	0.03	6	4
ON	Spikes	Dynamic Clamp	0.67	0.31	2.0×10^{-3}	10	6

Table S1. Speed tuning indices, related to Figures 1-7

Speed tuning indices of DSGC inputs and outputs. Index values range from −1, which indicates preference for low velocities, to +1, which indicates preference for high velocities. Values tending toward zero indicate equal responses to high and low velocities. All P values are comparisons made to a zero median distribution via Wilcoxon signed-rank test.